

# Changes of metabolite profile in kainic acid induced hippocampal injury in rats measured by HRMAS NMR

Hui Mao · Donna Toufexis · Xiaoxia Wang ·  
Agnès Lacreuse · Shaoxiong Wu

Received: 9 March 2007 / Accepted: 4 July 2007  
© Springer-Verlag 2007

**Abstract** The solid-state high resolution magic angle spinning nuclear magnetic resonance (HRMAS NMR) technique was applied in this work to characterize and quantify the neurochemical changes in the rat hippocampus (CA1 or CA3) after local administration of kainic acid (KA). Intact tissue samples obtained from the KA treated and control brain samples were analyzed using HRMAS NMR. Metabolite profiles from NMR spectra of KA treated and control samples revealed the statistical significant decrease of *N*-acetylaspartate (NAA) and an increase of choline derivatives in the CA1 and CA3 directly receiving KA injection. Less extensive KA-induced metabolic changes were found in the hippocampi sample from the area contralateral to the site receiving KA administration. These results provided quantitative metabolic information on KA-induced neuronal loss and cell breakdown. In addition, the present study also revealed increased level of  $\gamma$ -aminobutyric acid (GABA) and glutamate after KA

treatment, suggesting that the cellular release of inhibitory and excitatory amino acids can be quantified using this method. KA induced microglia activation was evidenced by increased level of myo-inositol (myo-I). This study demonstrates that ex vivo HRMAS NMR is a useful tool for analyzing and quantifying changes of neurochemistry and cerebral metabolism in the intact brain.

**Keywords** Neurochemistry · Cerebral metabolism · Kainic acid · NMR · Hippocampus · Neurotransmitter · Brain injury

## Abbreviations

KA	Kainic acid
HRMAS	High resolution magic angle spinning
NMR	Nuclear magnetic resonance
MRS	Magnetic resonance spectroscopy
NAA	<i>N</i> -acetyl-aspartate
Cho	Choline
PC	Phosphocholine
GPC	Glycerophosphocholine
Cre	Creatine
myo-I	Myo-inositol
Glu	Glutamate
Gln	Glutamine
GABA	$\gamma$ -aminobutyric acid
DANTE	Delays alternating with nutations for tailored excitation

H. Mao (✉) · X. Wang  
Department of Radiology and Frederick Philips MR  
Research Center, Emory University School of Medicine,  
1364 Clifton Road, Atlanta, Georgia 30322, USA  
e-mail: hmiao@emory.edu

D. Toufexis · A. Lacreuse  
Yerkes National Primate Research Center,  
Emory University, Atlanta, Georgia 30322, USA

A. Lacreuse  
Department of Psychology,  
University of Massachusetts-Amherst,  
Amherst 01003, USA

S. Wu  
Department of Chemistry and Center of NMR Research,  
Emory University, Atlanta, Georgia 30322, USA

## Introduction

Kainic acid (KA) induced neurotoxic action in rats is widely used as an experimental model for studying neurotoxicity, apoptosis, brain injuries and epileptic seizures, as

well as other mechanisms related to the excitatory amino acid transmission (Sperk 1994; Ben-Ari et al. 1986; Tanaka and Simon 1994; Ermakova et al. 2005). A wide range of studies in the literature has demonstrated the potent excitatory effect of KA. Several mechanisms have been proposed to describe the KA induced brain damage in animal models, for example: (1) KA may cause direct axon-sparing lesions in the vulnerable brain areas after systemic or intracerebral injection; (2) KA may exert strong excitatory actions to cause seizures and distant (excitotoxic) brain damage in certain target neurons; (3) KA may lead to secondary seizure-related neuropathological events, such as hypoxia, hypoglycemia or edema. The hippocampus is known to be particularly vulnerable to excitotoxic agents such as KA. Experimental studies have shown that KA applied to the CA3 area of hippocampus can cause selective pyramidal cell death and activates microglial cells (Abraham et al. 2001). The selective vulnerability of hippocampal neurons can be explained by a possible increase in extracellular excitatory amino acids (Sperk 1994; Saransari and Oja et al. 1998). The high level of excitatory amino acids, released by direct application of KA, initiates NMDA receptor activation, neuronal depolarization and a very high rate of action potential firing, which may lead to neuronal cell death.

Although the histopathological and morphological information about the cell death after KA treatment can be readily studied, the neurochemical and metabolic changes associated with the event are difficult to obtain from animals *in vivo*. Nuclear magnetic resonance (NMR), also known as magnetic resonance spectroscopy (MRS) in its *in vivo* applications, is an analytic method that can identify and quantify chemicals. Since different metabolites display a unique set of signals at different chemical shifts, MRS can be used to profile the tissue metabolites in the selected sample volume *in vitro* and *in vivo*. Therefore, it is an attractive tool particularly for non-invasively studying neurochemistry and metabolism in living systems and has been applied in research and clinical diagnosis of various brain diseases (Ross et al. 1998).

Most of  $^1\text{H}$  MRS spectrum obtained from a brain *in vivo* typically consists of resonances attributed to the following key metabolites: *N*-acetylaspartate (NAA), myo-inositol (myo-I), choline and its derivatives (Cho), creatine (Cre), lactate (Lac), and glutamate/glutamine (Glx). NAA is found at the highest level in neurons in the normal brain and is considered as a neurochemical marker for neuron density (Tsai and Coyle 1995). NAA is typically reduced in diseases in which neuronal loss is evident. Myo-I, a cellular osmolyte, is considered as a marker for glia content and has been found to be elevated in pathological states where glia activation is prominent (Ross et al. 1997). The Cho resonances, often a sum of choline and its derivatives such as

phosphocholine (PC) and glycerophosphocholine (GPC), are related to the membrane metabolism and neurotransmission (Miller 1991). An increase in Cho derivative, or total choline, is considered to represent the metabolic processes associated with the high turnover of the cell membrane such as membrane breakdown, demyelination or inflammation. The resonance from Cre is composed of creatine and its derivative phosphocreatine and is related to the energy stores in the brain (Miller 1991). Lactate is the product of glycolysis, and is usually observed under hypoxic conditions. Major neurotransmitters, such as excitatory amino acids glutamate (Glu), glutamine (Gln) (Ross et al. 1997), can also be found in the spectra.

Non-invasive *in vivo* MRS has been used for studying neurochemical changes in response to KA treatment (Ebisu et al. 1994; Najm et al. 1997). It was found that KA administration caused a reduction in NAA/Cre ratio and an increase of total Cho derivatives in the rat brain. The ictal and early post-ictal increase in lactate/Cre ratio may reflect increased cellular activity and metabolism resulting from KA excitotoxicity. Detailed resonance assignments and quantitative measurement of neurochemical changes associated to the KA treatment were not available due to the low sensitivity and insufficient spectral resolution at the low magnetic field strength as well as experimental limitations with live animals. Alternatively, metabolite profiles of tissue samples obtained from biopsy specimens or sacrificed animals can be studied in detail using *ex vivo* high resolution NMR approaches, because of the superb sensitivity of this method to the low concentration metabolites and the improved resonance dispersion at the ultra high field strength. The solid-state high resolution magic angle spinning (HRMAS) NMR method uses intact tissue sample instead of the soluble extraction of the tissue (Cheng et al. 1997; Martinez-Bisbal et al. 2004) therefore, it offers additional advantages of retaining tissue morphology and eliminating contamination associated to the extraction procedure. Thus, it is a powerful tool to assist the interpretation and quantification of spectroscopic data. This method is especially suitable for studying the animal models in which the spectroscopic information can be obtained both *in vivo* and *ex vivo*.

The purpose of this study is to test if HRMAS NMR can be used to profile neurochemical changes associated to a neurological event. We have characterized the neurochemical changes caused by the KA treatment using intact tissue samples obtained from the control and KA treated animals. The detailed metabolite profiles of KA treated and control samples were investigated. The quantitative spectroscopic analysis revealed metabolic changes associated with KA induced neuronal loss including those of several excitatory and inhibitory amino acids and demonstrated that *ex vivo* HRMAS NMR is a useful tool for analyzing neurochemistry in the intact brain.

## Materials and methods

### Animal preparation and KA injections

Male Sprague-Dawley rats (250–300 g) were anesthetized under ketamine/xylazine (ketamine:100 mg/100 ml, xylazine:20 mg/ml at 1 ml/kg wt.) administrated intraperitoneally. For experimental animals ( $N = 6$ ), 0.5  $\mu\text{g}$  kainic acid (Sigma Chemical Co., St Louis, MO) dissolved in 0.5  $\mu\text{l}$  artificial CSF (aCSF) was injected into the right lateral ventricle by the stereotaxic injection. For control animals ( $N = 6$ ), only 0.5  $\mu\text{l}$  aCSF were injected into the right lateral ventricle using the same procedure applied for the experimental group. After injection, rats were allowed to recover from anesthesia and were monitored for seizure activity. Seven days later rats were anesthetized with isoflurane and immediately decapitated. The brain was snap frozen in dry ice and then immediately sliced into the 2 mm thick coronal section to obtain a section of the hippocampus (from Bregma  $-3.30$  to  $-5.30$ ). Sections containing the complete hippocampi were stored at  $-80^\circ\text{C}$  before NMR experiments.

### High resolution magic angle spinning nuclear magnetic resonance sample preparation

The intact tissue samples of the control and KA treated brain, approximately  $1 \times 1 \times 1.5 \text{ mm}^3$ , were cut off from hippocampi, i.e., both left and right CA1 and CA3 regions. Each sample was weighted (ranging from 31 to 38 mg) and then thawed in 99% saline  $\text{D}_2\text{O}$  before being loaded on the sample holder/rotor (4 mm  $\text{ZrO}_2$ ). After loading the tissue sample, a 50  $\mu\text{l}$  insert was placed in the sample holder to stabilize the sample and to provide the balance for the rotor.  $\text{D}_2\text{O}$  solvent was added to obtain frequency-lock signal for NMR experiments. The preparation of NMR samples was done rapidly on ice to avoid sample degradation. All samples were measured three times at  $4^\circ\text{C}$  during a 24-h period to check if there was any detectable degradation. The water resonance (4.65 ppm) was used as the internal reference for chemical shift. For external chemical shift reference, aliquot amount of tetramethylsilane,  $(\text{CH}_3)_4\text{Si}$ , (TMS) was added in the selected samples.

### High resolution magic angle spinning nuclear magnetic resonance data acquisition

High resolution magic angle spinning nuclear magnetic resonance experiments were conducted at  $4^\circ\text{C}$  using a Bruker AVANCE 600 WB solid state NMR spectrometer (Bruker Instruments, Inc.) with a dedicated 4 mm HRMAS probe. The probe-head was pre-cooled to  $4^\circ\text{C}$  before loading the sample. The sample/probe temperature was main-

tained throughout the experiment ( $\pm 0.1^\circ\text{C}$ ) via a variable temperature control unit. Sample spinning rates were controlled in the range of 2,800 KHz ( $\pm 2$  Hz) or at lower spin rate of 800 Hz if the rotor-synchronized delay alternating with nutation for tailored excitation (DANTE) sequence (Morris and Freeman 1978) was used. This sample spin rate was tested to ensure the spin sidebands not affecting the spectrum. Spectra were acquired with and without suppression of water signal. The presaturation of water was achieved with a zqpr sequence before acquisition pulses. A rotor-synchronized Carr–Purcell–Meibom–Gill (CPMG) pulse sequence  $(90-(\tau-180-\tau)_n)$  acquisition) was used to function as a  $T_2$  filter to suppress broad signals from macromolecules. The inter-pulse delay ( $\tau = 2\pi/\omega_r$ ) was synchronized with the rotor rotation ( $\tau$  indicates the sample spinning rate in time units and  $\omega_r/2\pi$  represents the spinning rate in kHz). The value of  $n$  for each sample was adjusted to create a  $T_2$  filter of  $2n\tau = 50 \text{ m}$ . The pulse length of  $90^\circ$  is calibrated and adjusted based on each sample. The number of transients was 256. A repetition time was 5.0 s and a spectral width was 10 kHz in all experiments. This procedure was adapted from that used in the other studies (Cheng et al. 1997; Swanson et al. 2003). The data were processed using software implemented on the instrument. Line broadening (1 Hz) apodization was applied to all free induction decays (FIDs) before Fourier transformation. Regional integrals of the metabolites from 0.5 to 4.5 ppm were measured for the calculation of metabolite concentrations.

For resonance assignment and confirmation, two-dimensional (2D)  $^1\text{H}$  J-coupled total correlated spectroscopy (TOCSY) was used. A DIPSI-2 mixing sequence for homonuclear Hartman–Hahn transfer implemented on the instrument was used for data acquisition with 170 m acquisition time, 50 m spin lock duration, 6,000 Hz spectral width, and 1.5 s relaxation delay. Thirty-two transients were averaged for each of the 256 increments with a total acquisition time of  $\sim 4$  h. 2D spectral data were analyzed on the instrument using zero filling to a  $2\text{k} \times 2\text{k}$  matrix and weighted with a shifted square sine bell function followed by Fourier transformation.

### Metabolite assignment and quantification

Chemical shift values of the resonances of interests were determined using external reference of  $-\text{CH}_3$  protons of TMS as (0 ppm at  $4^\circ\text{C}$ ) when TMS was added, or using internal references of proton resonances of  $\text{H}_2\text{O}$  at (4.65 ppm) or  $-\text{CH}_3$  of NAA (2.02 ppm). Resonance assignments for the metabolites of interest were obtained based on their chemical shifts reported in the literatures and were further confirmed by 2D TOCSY spectra collected in this study. For calculating the concentrations of

metabolites of interest from NMR spectra, peak integrals of the selected resonance of each metabolite were measured and then calibrated to the peak integral of the external reference of TMS. The concentration of each metabolite was then calculated based on the sample wet weight and the concentration of TMS in the sample, assuming that tissue water and TMS concentration is stable during the NMR experiment.

### Statistical analysis

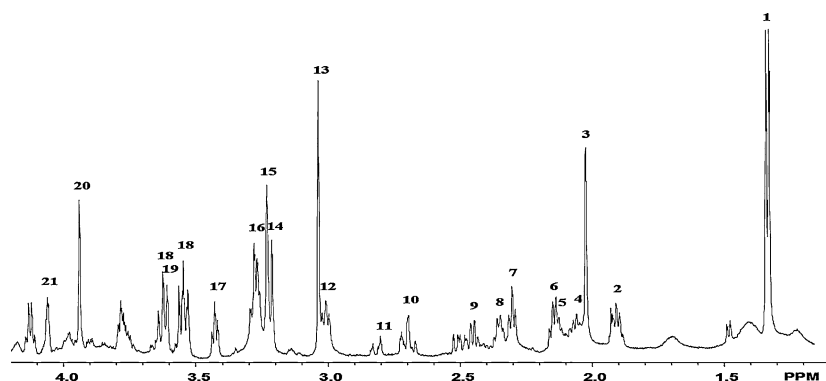
Spectral measurements were averaged and expressed as mean standard deviation ( $\pm$ SD). Statistical differences were analyzed using Student's *t*-test (SigmaStat 3.0; Systat Software). The differences in metabolite ratios between controls and KA treated samples were analyzed using one-way ANOVA. Statistical correlations were analyzed using Pearson (parametric) test and a value of  $P < 0.05$  is considered to be statistically significant.

## Results

### Sample stability under experimental conditions

The metabolite profile of preserved tissue samples was investigated for possible changes due to the sample degradation and contamination under the HRMAS NMR experimental condition. The same sample was repeatedly tested, restored and retrieved at different times, i.e., 1, 4, 12, 24, 72 and 140 h. Except for the lactate resonance, which increased by 20% after 72 h, the spectra obtained at different times showed almost no change in all key metabolites before and after a typical 24-h experiment session. This result indicated that the sample preservation condition and the experimental condition did not cause the sample degradation that affects the data quality. For all other experiments, spectra of each sample were collected in the beginning and the end of NMR experiments.

**Fig. 1** A selected region of one-dimensional (1D) HRMAS NMR spectrum from a rat hippocampus sample (CA1). The protons from metabolites are numbered with their chemical shift values listed in Table 1



### Metabolite assignments and profiles

Highly resolved NMR spectra were obtained from all samples. Figure 1 shows one of the NMR spectra from KA treated samples. The chemical shifts of resonances from metabolites of interest are listed in the Table 1. Most of the resonance assignments are in good agreement with those reported previously (Griffin et al. 2002; Martinez-Bisbal et al. 2004; Tong et al. 2004; Tsang et al. 2005). 2D TOCSY spectra (shown in Fig. 2) confirmed the assignment of the spin systems of glutamine and glutamate, based on the J-coupling correlations.

Metabolite profiles revealed following characteristics of KA induced neurochemical changes. As shown in Fig. 3, NAA (2.02 ppm) decreased in the KA treated hippocampi samples compared to the control samples. Cho derivatives (Cho, PC and GPC), particularly PC (~3.23 ppm), increased in KA treated samples compared to the control samples. Furthermore, increase of Cho derivatives and decrease of NAA were more pronounced in the sites ipsilateral to the injection (CA1\* and CA3\*) compared to the sites in the contralateral hemisphere. Decreased NAA was coupled with substantial increase of acetate (Ace, 1.93 ppm) in the spectra of the KA treated hippocampi. Noticeable increase of GABA (e.g.,  $-\text{CH}_3$ , 1.91 ppm and  $-\text{CH}_2$ , 2.31 ppm) was observed in the KA treated samples. In addition, there were mild increases of various amino acids, such as glutamate and aspartate, in the KA treated samples. Furthermore, spectroscopic analysis showed that the KA treatment also induced increase of myo-I resonances (e.g., 3.27 and 3.55 ppm).

### Metabolite quantification

Highly resolved spectra and availability of internal ( $\text{H}_2\text{O}$ ) and external (TMS) references allowed us to calculate the metabolite concentrations in the sample. The concentration was normalized to the level of Cre in the control sample since Cre level is the least varied in the sample. Changes of several metabolites of interest, e.g., NAA, Cre, Cho

**Table 1** Resonance assignments and averaged metabolite concentrations in the control samples ( $N = 6$ )

Peak no	Metabolite	$^1\text{H}$ or spin <sup>a</sup>	Chemical shift (ppm)	Concentration mM (SD) <sup>b</sup>
1	Lactate	$-\text{CH}_3$	1.34	$16.28 \pm 1.08$
2	$\gamma$ -aminobutyric acid (GABA)	$-\text{CH}_3$	1.90	$5.28 \pm 0.37$
3	<i>N</i> -acetyl-aspartate (NAA)	$-\text{CH}_3$	2.02	$13.37 \pm 0.41$
4	Glutamate (Glu)	$-\text{CH}_3$	2.07	
5	Glutamine (Gln)	$\beta$ - $\text{CH}_2$	2.14	
6	Glutamine(Gln)	$-\text{CH}_3$	2.15	
7	$\gamma$ -aminobutyric acid (GABA)	$\beta$ - $\text{CH}_2$	2.31	
8	Glutamate (Glu)	$\gamma$ - $\text{CH}_2$	2.36	$4.64 \pm 0.38$
9	Glutamine (Gln)	$\gamma$ - $\text{CH}_2$	2.45	$4.23 \pm 0.45$
10	<i>N</i> -acetyl-aspartate (NAA)	$\beta$ - $\text{CH}_2$	2.70	
11	Aspartic acid	$\beta$ - $\text{CH}_2$	2.81	$1.37 \pm 0.11$
12	$\gamma$ -aminobutyric acid (GABA)	$\delta$ - $\text{CH}_2$	3.02	
13	Creatine (Cre)	$-\text{CH}_3$	3.04	$14.26 \pm 0.42$
14	P-choline (PC)	<i>N</i> - $(\text{CH}_3)_3$	3.22	$3.64 \pm 0.22$
15	Glyocerphosphocholine (GPC)	<i>N</i> - $(\text{CH}_3)_3$	3.24	$4.01 \pm 0.18$
16	Myo-insitol (myo-I)	$-\text{CH}-(5)$	3.27	$7.21 \pm 0.55$
17	Taurine	$-\text{CH}_2$ - $\text{SO}_3$	3.43	$7.58 \pm 0.21$
18	Myo-insitol (myo-I)	$-\text{CH}-(1)$	3.55	
19	Myo-insitol (myo-I)	$-\text{CH}-(3)$	3.63	
20	Creatine (Cre)	$-\text{CH}_2$	3.95	
21	Myo-insitol (myo-I)	$-\text{CH}-(2)$	4.07	

<sup>a</sup> The resonance assignments were referenced to the previous reported (Martinez-Bisbal et al. 2004)

<sup>b</sup> The concentration of each metabolite then was calculated based on the sample wet weight and the concentration of TMS in the sample, assuming that tissue water and TMS concentration is stable during the NMR experiment. Peak integral was measured and used in the calculation

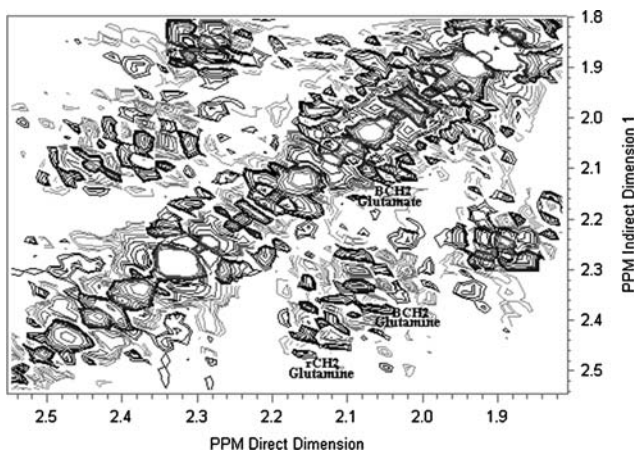


**Fig. 2** An expanded region of 2D TOCSY spectrum showed cross-peaks of J-coupled  $-\text{CH}_2$  of glutamate

derivatives, amino acids and myo-I, were semi-quantified in the KA treated samples and were obtained by comparing the concentrations to those of the control samples. The extent of the KA effect to metabolite profiles was indicated by the change in the ratios of metabolite/Cre. It should be noted that the tissue injury as a result of the needle penetration might potentially cause neurochemical changes at the site of injection, even though it was not observed in the pre-

vious studies. In our study, spectra recorded from the site receiving aCSF injection and from its contralateral site of control brains did not show a statistically significant difference. Therefore, metabolite concentrations of control samples were averaged from all CA1 and CA3 locations, i.e., aCSF injection sites and contralateral sites. Table 2 summarized changes of metabolite levels in different regions of hippocampus after the KA treatment when compared to controls. In general, there is a statistical significant difference ( $P = 0.0085$ ) between control and KA treated samples. The changes of Cho derivatives, NAA and acetate were most noticeable. For instances, the ratio of NAA/Cre decreased remarkably from 1.20 in the control samples to 0.38 in the CA1\* (KA injected site) and 0.84 in the CA1 (contralateral site) of KA treated brains, respectively. Similarly, NAA/Cre decreased to 0.39 in the CA3\* and 0.72 in the contralateral CA3 of KA treated brains versus 1.20 in the control samples. The reduction of NAA was coupled with the appearance and increase of acetate in the samples of KA treated brain. PC/Cre showed substantial increase in the KA treated areas, from 0.22 in the control samples to 0.45 in the CA1\* and 0.58 in the CA3\* of treated samples, respectively. However, Cho/Cre changed only slightly. PC/Cre was also elevated in the site contralateral to KA injection site.

Kainic acid induced increase of various excitatory amino acids, such as glutamate, aspartate, and inhibitory neuro-

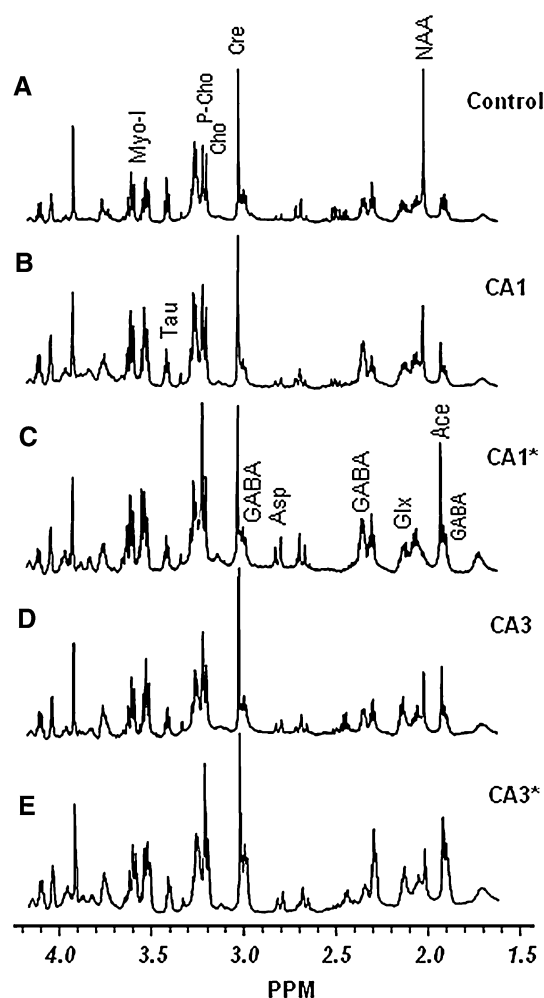


**Fig. 3** A set of HRMAS NMR spectra of tissue samples from the hippocampi sections of a non-treated (a) and a kainic acid-treated rat (b–e). Samples from the treated hemisphere were indicated with \*. Chemical shift is referenced at 4°C

transmitter GABA, were quantified. Most noticeable observation was that the ratio of GABA/Cre was increased from 0.27 in the control samples to 0.46 and 0.54 in the KA treated CA1\* and CA3\*.

**Table 2** KA induced changes of selected metabolites in different hippocampal samples

Metabolite	Chemical shift	Metabolite/Cre				Non-treated control Ave. CA1 & CA3
		KA treated		Contralateral site		
		CA1*	CA3*	CA1	CA3	
GABA	1.90	0.46	0.54	0.47	0.43	0.27
Ace	1.93	1.18	1.21	0.59	0.67	0.04
NAA	2.02	0.38	0.39	0.84	0.72	1.20
Glu	2.08	0.43	0.64	0.47	0.35	0.27
Gln	2.14	0.16	0.26	0.20	0.18	0.23
Asp	2.81	0.53	0.54	0.45	0.38	0.23
Cho	3.21	0.24	0.27	0.30	0.32	0.21
PC	3.23	0.45	0.58	0.35	0.39	0.22
myo-I	3.27	1.16	1.27	1.00	1.04	0.88

The level of individual metabolite was normalized in relation to that of Cre, and presented as metabolite/Cre

## Discussion

### Kainic acid induced neurochemical changes

It is widely recognized that local administration of KA induces neuronal degenerations, especially in the pyriform and entorhinal cortices. Hippocampus CA1 and CA3 are mostly susceptible to the effect of KA treatment, followed by general tissue necrosis, especially in the pyriform cortex. The example found in the previous work (Dudek et al. 2002) showed that the KA injection produced neuronal loss and reactive gliosis in both CA1 and CA3 on the injected side relative to the control side, and relative to the same hippocampal regions of untreated control rats. Our data from HRMAS NMR revealed the significant decrease of NAA, an indication of neuronal loss, and increase of Cho, often associated with the high membrane turnover rate and cell breakdown, in the KA treated CA1\* and CA3\*. HRMAS NMR data in the present study provided the quantitative analysis of the neuronal loss or severity of the KA effect using endogenous NAA and Cho concentrations as indicators. Furthermore, our experiments also demonstrated that local administration of KA may affect the CA1 and CA3 regions contralateral to the injection site in the KA treated brain. This is evidenced by the decreased NAA and increased Cho in the samples of those regions relative to the CA1 and CA3 samples from untreated control animals. Such change of the metabolite profile is similar to that of KA directly treated side. However, the KA induced neurochemical changes in the contralateral sites were not as severe as those in the injection sites. There are considerable evidences suggesting that not only a direct neurotoxic action of KA but also presumably sustained stimulation of excitatory pathways in the brain may cause brain damage in KA-induced seizures. Therefore, our observation of metabolic changes in the contralateral hippocampus may be the result of the seizure-induced excitotoxicity, although other possible mechanisms may also be involved.

Previous *in vivo* MRS study of KA treated rats showed the changes in NAA/Cr and Lac/Cr ratios during the postictal and interictal phases and up to 24 h after the injection of KA. The prolonged lactate/Cr increase in an area susceptible to neuronal damage (e.g., hippocampus) correlated with the onset of seizure activity but remained elevated thereafter. It was concluded that the ictal and early postictal increase in lactate may reflect increased cellular activity and metabolism resulting from KA excitotoxicity. The observation of ictal increase in NAA/Cr ratio was explained as the possible activation of the *N*-acetylaspartylglutamate (NAAG) dipeptidase pathway and the late postictal decrease in NAA/Cr ratios as a reflection of KA induced neuronal cell loss. Since our study was conducted 7 days after animals received KA administration, our observation of decrease of NAA/Cr is consistent with that of the postictal effect. Because of our concern that lactate level may not be truly represented in the postmortem samples, we decided not to use lactate as the measurement of KA induced changes.

Interestingly, the high resolution of HRMAS NMR was able to resolve Cho, PC and GPC resonances, which mostly overlap in the spectra recorded at the lower field, allowing for quantifying choline derivatives individually. Our data suggested that PC was elevated in KA treated samples as shown in PC/Cr ratio, whereas the change of Cho was not pronounced. Increase of the total choline is often considered to be associated with the high turnover rate of cell membrane. However, the roles of individual choline species in responding to the KA treatment remain to be further studied.

#### Involvement of excitatory amino acids and inhibitory GABA

Excitatory amino acids such as glutamate and the inhibitory neurotransmitter GABA are considered to be involved in mediating neuronal stimulation during epileptic events such as KA induced seizure (During and Spencer 1993; Yager et al. 2002; Bianchi et al. 2003; Ding et al. 1998). HRMAS NMR data from this work showed increased glutamate, aspartate and GABA in the KA treated samples compared to the controls.

Traditionally, extracellular amino acids can be measured using microdialysis technique and HPLC from samples extracted from CSF (Bruhn et al. 1997; Takeda et al. 2003). HRMAS NMR measurement of glutamine, glutamate, aspartate and GABA represents the concentration of amino acids in the intact tissue and does not involve homogenizing the samples and multiple steps of sample preparations with various reagents. It is noticed that data from the current study showed much higher concentrations of amino acids, e.g., 4.64 mM of Glu and 5.28 mM of GABA mea-

sured by HRMAS NMR in this study comparing to 10–50  $\mu$ M range of glutamate and GABA measured by microdialysis (Ding et al. 1998; Liu Z et al. 1997). This is likely because HRMAS NMR measures both intracellular and extracellular metabolites with the majority as intracellular components, whereas microdialysis method measures only the chemicals released to the extracellular space. Therefore, HRMAS NMR method may be a useful tool to provide insight of intracellular activity and capacity of neurotransmitter systems.

#### Metabolic evidence of KA induced microglial activation

Previous studies of microglial reaction following ischemic hypoxia or KA administration suggested that the neuronal death caused by the KA treatment may be preceded by the activation of microglia (Jorgensen et al. 1993; Mitchell et al. 1993; Taniwaki et al. 1996). Our results showed mild increase of myo-inositol in the KA treated samples, i.e., 12% at the injected sites ( $P = 0.054$ ) and 7% at contralateral sites ( $P = 0.071$ ), compared to the control samples from brains without KA treatment. Myo-I plays a role of osmolyte and is also suggested to be a marker for glia content as it has been found to be elevated in pathological states where glial activation is prominent (Ross et al. 1997). As the previous studies using different methods, such as the extracellular recording of cortical slices, reported that KA treatment was associated with enhanced glial activity, our observation of the increase of myo-I in KA treated animals compared to controls may indicate elevated glia content after the treatment. However, we cannot rule out the possible change in osmotic environment after KA-induced seizure and injury.

#### Advantage of HRMAS NMR method

There are limited methods for studying neurochemical changes *in vivo*. The 2-deoxyglucose method (Sokoloff et al. 1981) has been used for investigating metabolic activity during and after KA induced seizures. The time-course and regional distribution of local glucose consumption were found to be correlated to the high seizure activity and the pattern of neuronal damage (Ben-Ari et al. 1981; Tremblay et al. 1983). It was reported that the CA3 area of the hippocampus was the most sensitive to KA effect, as evidenced by accumulation of 2-deoxyglucose after KA treatment. Microdialysis is the other commonly used technique to investigate the release of neurochemicals, including excitatory amino acids, during and after KA treatment (Liu et al. 1997; Bruhn et al. 1997). However, this method demands the accurate placement of an invasive intracranial probe and the chromatography analysis of extracted CSF samples.

Magnetic resonance spectroscopy method has been widely used in research and clinical diagnosis of various brain diseases using specific metabolites as “surrogate markers” representing the presence of particular cell types. It provides insights into metabolic processes non-invasively for monitoring treatment responses or disease progression. Previous *in vivo* MRS study of seizure activities in KA treated rats showed that changes in NAA/Cr and Lac/Cr ratios could be investigated in live animals repeatedly. However, to develop non-invasive *in vivo* application of MRS, one critical step is to test and validate the method and data using *ex vivo* histological or analytical analysis. HRMAS NMR analysis is already established and widely accepted in the fields of chemistry and biochemistry as a primary method for characterization and profiling of chemicals in the materials. Its application has been recently extended to the metabolite profiling of pathology and diseases, such as tumors from brain, prostate and breast and other organs, using tissue specimens obtained from biopsy or surgery. Analyzing tissue specimens obtained from biopsied or sacrificed animals using high resolution NMR *ex vivo* can be a powerful method to validate the *in vivo* MRS data, since it permits remarkable high spectra resolution and sensitivity. It can be used to assist the interpretation and quantification of spectra obtained *in vivo* and to characterize unknown or newly discovered resonances or chemicals. Because of the superb sensitivity of this method to the low concentration metabolites and the improved spectral resolution or resonance peak dispersion at the ultra high field strength, we were able to obtain high resolution metabolite profiles and to quantify each key metabolites using the *ex vivo* high resolution NMR approach. Such quantified data and ability to examine KA induced changes in individual metabolites were not available in the previous studies. Our study demonstrated that this method is especially suitable for studying animal models in which the spectroscopic information can be obtained both *in vivo* and *ex vivo*.

## Conclusion

High resolution *ex vivo* HRMAS NMR was able to detect and quantify changes in hippocampal neurochemistry following the KA treatment. HRMAS NMR analysis of intact rat hippocampi revealed the significant decrease of *N*-acetylaspartate and increase of choline derivative, phosphocholine, in the KA treated CA1\* and CA3\*. Furthermore, KA induced metabolic changes, although less extensive, were also found in the hippocampi samples from the areas contralateral to the sites that received KA administration directly. Quantitative spectroscopic analysis demonstrated that the KA administration led to the increase of

$\gamma$ -aminobutyric acid and glutamate, suggesting the releases of excitatory and inhibitory amino acids. KA induced activation of microglia is evidenced by observation of increased myo-inositol. Given its high spectral resolution for intact tissue samples, this study demonstrate that HRMAS NMR is a powerful tool for profiling and identifying the metabolic markers of the neural and glial alterations, which can be potentially used in the *in vivo* application of MRS in living animals and human.

## References

- Abraham H, Losonczy A, Czeh G, Lazar G (2001) Rapid activation of microglial cells by hypoxia, kainic acid, and potassium ions in slice preparations of the rat hippocampus. *Brain Res* 906:115–126
- Ben-Ari Y, Riche D, Tremblay E, Cherton G (1981) Alterations in local glucose consumption following systemic administration of kainic acid, bicuculline or metrazol. *Eur Neurol* 20:173–175
- Ben-Ari Y, Repressa A, Tremblay E, Nitecka L (1986) Selective and non-selective seizure related brain damage produced by kainic acid. *Adv Exp Med Biol* 203:647–657
- Bianchi L, Ballini C, Colivicchi MA, Della Corte L, Giovannini MG, Pepeu G (2003) Investigation on acetylcholine, aspartate, glutamate and GABA extracellular levels from ventral hippocampus during repeated exploratory activity in the rat. *Neurochem Res* 28:565–573
- Bruhn T, Christensen T, Diemer NH (1997) Evidence for increased cellular uptake of glutamate and aspartate in the rat hippocampus during kainic acid seizures. A microdialysis study using the “indicator diffusion” method. *Epilepsy Res* 26:363–371
- Cheng LL, Ma MJ, Becerra L, Ptak T, Tracey I, Lackner A, Gonzalez RG (1997) Quantitative neuropathology by high resolution magic angle spinning proton magnetic resonance spectroscopy. *Proc Natl Acad Sci USA* 94:6408–6413
- Ding R, Asada H, Obata K (1998) Changes in extracellular glutamate and GABA levels in the hippocampal CA3 and CA1 areas and the induction of glutamic acid decarboxylase-67 in dentate granule cells of rats treated with kainic acid. *Brain Res* 800:105–113
- Dudek FE, Hellier JL, Williams PA, Ferraro DJ, Staley KJ (2002) The course of cellular alterations associated with the development of spontaneous seizures after status epilepticus. *Prog Brain Res* 135:53–65
- During MJ, Spencer DD (1993) Extracellular hippocampal glutamate and spontaneous seizure in the conscious human brain. *Lancet* 341:1607–1610
- Ebisu T, Rooney WD, Graham SH, Weiner MW, Maudsley AA (1994) *N*-acetylaspartate as an *in vivo* marker of neuronal viability in kainate-induced status epilepticus:  $^1\text{H}$  magnetic resonance spectroscopic imaging. *J Cereb Blood Flow Metab* 14:373–382
- Ermakova IV, Loseva EV, Hodges H, Sinden J (2005) Transplantation of cultured astrocytes attenuates degenerative changes in rats with kainic acid-induced brain damage. *Bull Exp Biol Med* 140:677–681
- Griffin JL, Bollard M, Nicholson JK, Bhakoo K (2002) Spectral profiles of cultured neuronal and glial cells derived from HRMAS  $^1\text{H}$  NMR spectroscopy. *NMR Biomed* 15:375–384
- Jorgensen MB, Finsen BR, Jensen MB, Castellano B, Diemer NH, Zimmer J (1993) Microglial and astroglial reactions to ischemic and kainic acid-induced lesions of the adult rat hippocampus. *Exp Neurol* 120:70–88
- Liu Z, Stafstrom CE, Sarkisian MR, Yang Y, Hori A, Tandon P, Holmes GL (1997) Seizure-induced glutamate release in mature and

- immature animals: an in vivo microdialysis study. *Neuroreport* 8:2019–2023
- Martinez-Bisbal MC, Marti-Bonmati L, Piquer J, Revert A, Ferrer P, Llacer JL, Piotta M, Assemat O, Celda B (2004)  $^1\text{H}$  and  $^{13}\text{C}$  HR-MAS spectroscopy of intact biopsy samples ex vivo and in vivo  $^1\text{H}$  MRS study of human high grade gliomas. *NMR Biomed* 17:191–205
- Miller BL (1991) A review of chemical issues in  $^1\text{H}$  NMR spectroscopy: *N*-acetyl-L-aspartate, creatine and choline. *NMR Biomed* 4:47–52
- Mitchell J, Sundstrom LE, Wheal HV (1993) Microglial and astrocytic cell responses in the rat hippocampus after an intracerebroventricular kainic acid injection. *Exp Neurol* 121:224–230
- Morris GA, Freeman R (1978) Selective excitation in Fourier transform nuclear magnetic resonance. *J Magn Reson* 29: 433–462
- Najm IM, Wang Y, Hong SC, Luders HO, Ng TC, Comair YG (1997) Temporal changes in proton MRS metabolites after kainic acid-induced seizures in rat brain. *Epilepsia* 38:87–94
- Ross BD, Bluml S, Cowan R, Danielsen E, Farrow N, Gruetter R (1997) In vivo magnetic resonance spectroscopy of human brain: the biophysical basis of dementia. *Biophys Chem* 68:161–172
- Ross BD, Bluml S, Cowan R (1998) In vivo MR spectroscopy of human dementia. *Neuroimaging Clin N Am* 8:809–822
- Saransaari P, Oja SS (1998) Release of endogenous glutamate, aspartate, GABA, and taurine from hippocampal slices from adult and developing mice under cell-damaging conditions. *Neurochem Res* 23:563–570
- Sokoloff L (1981) Localization of functional activity in the central nervous system by measurement of glucose utilization with radioactive deoxyglucose. *J Cereb Blood Flow Metab* 1:7–36
- Sperk G (1994) Kainic acid seizures in the rat. *Prog Neurobiol* 42:1–32
- Swanson MG, Vigneron DB, Tabatabai ZL, Males RG, Schmitt L, Carroll PR, James JK, Hurd RE, Kurhanewicz J (2003) Proton HR-MAS spectroscopy and quantitative pathologic analysis of MRI/3D-MRSI-targeted postsurgical prostate tissues. *Magn Reson Med* 50:944–954
- Takeda A, Hirate M, Tamano H, Oku N (2003) Release of glutamate and GABA in the hippocampus under zinc deficiency. *J Neurosci Res* 72:537–542
- Tanaka K, Simon RP (1994) The pattern of neuronal injury following seizures induced by intranigral kainic acid. *Neurosci Lett* 176:205–208
- Taniwaki Y, Kato M, Araki T, Kobayashi T (1996) Microglial activation by epileptic activities through the propagation pathway of kainic acid-induced hippocampal seizures in the rat. *Neurosci Lett* 217:29–32
- Tong Z, Yamaki T, Harada K, Houkin K (2004) In vivo quantification of the metabolites in normal brain and brain tumors by proton MR spectroscopy using water as an internal standard. *Magn Reson Imaging* 22:1017–1024
- Tremblay E, Ottersen OP, Rovira C, Ben-Ari Y (1983) Intra-amygdaloid injections of kainic acid: regional metabolic changes and their relation to the pathological alterations. *Neuroscience* 8:299–315
- Tsai G, Coyle JT (1995) *N*-acetylaspartate in neuropsychiatric disorders. *Prog Neurobiol* 46:531–540
- Tsang TM, Griffin JL, Haselden J, Fish C, Holmes E (2005) Metabolic characterization of distinct neuroanatomical regions in rats by magic angle spinning  $^1\text{H}$  nuclear magnetic resonance spectroscopy. *Magn Reson Med* 53:1018–1024
- Yager JY, Armstrong EA, Miyashita H, Wirrell EC (2002) Prolonged neonatal seizures exacerbate hypoxic-ischemic brain damage: correlation with cerebral energy metabolism and excitatory amino acid release. *Dev Neurosci* 24:367–381